MIT 2295-80-1

FLAME LUMINOSITY AND UNBURNED HYDROCARBON MEASUREMENTS IN SWIRLING COMBUSTION

TOPICAL REPORT

by

A.J. GIOVANETTI, D.P. HOULT, J.C. KECK, AND A.F. SAROFIM

July 1980

Prepared for the U.S. DEPARTMENT OF ENERGY
under Contract EX-76-A-01-2295

THE ENERGY LABORATORY

Massachusetts Institute of Technology
Cambridge, Massachusetts 02139

Report No. MIT 2295-80-1

Distribution Category:

Principal Alternate
Fuels Program

FLAME LUMINOSITY AND UNBURNED HYDROCARBON MEASUREMENTS IN SWIRLING COMBUSTION

Topical Report

by

A.J. Giovanetti, D.P. Hoult, J.C. Keck, and A.F. Sarofim

The Energy Laboratory
Massachusetts Institute of Technology
Cambridge, Massachusetts 02139

Prepared for the U.S. Department of Energy
under Contract EX-76-A-01-2295

TABLE OF CONTENTS

LIST OF FIGURES

LIST OF TABLES

ACKNOWLEDGMENT

A note of appreciation goes to Mr. Steve Lanier of the U.S. Environmental Protection Agency Combustion Research Section, Research Triangle Park, North Carolina for his effort in securing the sample of distillate shale oil used in this research.

FLAME LUMINOSITY AND UNBURNED HYDROCARBON MEASUREMENTS IN SWIRLING COMBUSTION

by

A.J. Giovanetti, D.P. Hoult, J.C. Keck, and A.F. Sarofim

ABSTRACT

The relationship between flame luminosity and unburned hydrocarbon concentration was studied using an atmospheric, tubular burner. Spectroscopic studies were conducted for different fuels, including kerosene, nitrogen-doped kerosene, and shale oil. Independent exhaust gas analyses were performed on shale oil and nitrogen-doped kerosene.

At a particular fuel equivalence ratio, measurements showed flame luminosity to be a function of unburned hydrocarbons. Unburned hydrocarbons were found to become significant prior to an equivalence ratio corresponding to the flame's change from blue to yellow. This critical condition is a function of fuel-air mixing and inlet air preheat temperature.

Spectroscopic work revealed presence of strong carbon, hydrocarbon, amine, and cyanide band spectra for the nitrogen-containing fuels. Exhaust gas analyses for shale oil and a comparable nitrogen-doped kerosene were similar.

1. INTRODUCTION

The electromagnetic radiation emitted from a combustor is indicative of exhaust gas species present. Optical analysis of flame radiation would seem to be the thorough way of analyzing exhaust gas species. Most work to date employs insertion of a probe into the combustion zone and extraction of a physical sample which is then analyzed using dry or wet chemical techniques. The chemical techniques provide accurate

quantitative measurement of species concentrations, but they do have the disadvantage of yielding only time-averaged values. The possibility of disturbing the flow with the probe always exists.

Photometric studies could provide quantitative data on the space and time variation of species present. Optical techniques are a fast and efficient means to explore a wide range of burner operating conditions. They have the potential to become part of a feedback control system coupled to the burner to optimize combustion. Optical diagnostics could supply information regarding chemical kinetics of combustion.

Overall flame luminosity is an important indication of soot loading in a flame [1]. Luminous yellow flames contain substantial soot. In addition, Foster [2] showed for the combustion of fuels with high nitrogen content that luminous yellow flames yielded high concentrations of unburned hydrocarbons and hydrogen cyanide (HCN). Figure 1 shows HCN to correlate with unburned hydrocarbons. Further, Blazowski et al. [3] suggest control of both NO_x and soot requires operation of a combustor at the highest fuel-air ratio prior to the onset of significant hydrocarbons. In the case of highly aromatic fuels, this "hydrocarbon breakthrough" occurs simultaneously with the appearance of measurable soot in the flame. Adjustment of burner equivalence ratio to the point just prior to the appearance of a luminous yellow flame would control both soot formation and fuel nitrogen conversion. The application of this diagnostic has importance since coal derived fuels have high aromaticity (i.e., low sooting limit) and substantial fuel nitrogen [2,3].

A goal of this work is to explore the possibility of an empirical relation between overall flame luminosity and unburned hydrocarbons. Such a relation could be used as part of a control strategy for HCN and soot.

Qualitative spectroscopic studies will be used to identify band spectra present in the combustion products. It is important to know what species can be observed in a given flame condition, and if a particular flame condition inhibits observation of certain species present.

Independently, exhaust gas analyses utilizing dry and wet chemical techniques will be used to compare combustion of nitrogen-doped kerosene with a shale derived oil of similar composition. The goal of this later experiment is to determine if NO_x control strategies based on doped fuels hold for real synthetic fuels.

This report is organized as follows: Section 2 outlines the experimental burner, instrumentation, and fuels used. Sections 3 and 4 present and discuss the experimental results.

2. EXPERIMENTAL APPARATUS AND PROCEDURE

2.1 Continuous, Turbulent Combustor

The combustion facility used for all experiments was essentially that developed by Foster [2]. A schematic of the entire installation and a cross section of the burner tube are shown in Figures 2 and 3, respectively. The facility permits independent variation of four parameters: primary air flow, fuel flow, primary inlet air temperature, and fuel atomization pressure (mixing intensity).

The 0.10 m diameter cylindrical, two-stage burner is horizontally fired at atmospheric pressure. Liquid fuel is burned at a rate of 3.81×10^4 J/s resulting in a combustion intensity of 1.03×10^7 J/m^3-s-atm. Primary air flow is held constant at 0.0139 kg/s while dilution air to the afterburner is kept at 0.0069 kg/s. Reference to mixture conditions in this report refer to the main stage of the burner. Upstream of the burner is a thermostatically controlled 85 kW electric air preheater capable of heating primary and afterburner inlet air to 700°K.

As shown in Figure 3, the burner section closest to the nozzle has three 0.64 cm diameter optical ports spaced at one-half burner diameter intervals. Each port is open to the atmosphere and radially opposed by a similar port which permits observation of the flame with minimum wall radiation interference. Individual ports are fitted with steel plugs when not in use.

2.2 Exhaust Gas Instrumentation

Figure 4 depicts the exhaust gas sampling system used. Details of the system are found in [2].

2.3 Optical Instrumentation

Flame luminosity studies were conducted using the installation depicted in Figure 5. The experimental apparatus permits measurement of unburned hydrocarbon concentration 5.0 diameters downstream of the nozzle, determination of relative flame luminosity, and photographic record of each flame.

The optical system consists of a Canon model AT-1 35mm single-lens-reflex camera, Canon model FD 300mm f/5.6 S.S.C. telephoto lens, Canon model M bellows, and rear surface plane mirror. Standard ASA 100 Kodacolor II color negative film is used. In all runs, the camera is focused on the burner swirler vanes.

Total flame luminosity is measured using the camera's built-in exposure meter. The camera utilizes a cadmium-sulfide photocell and the central emphasis metering system [4]. Because there is depth to the flame in the axial direction, all luminosity measurements are integrated along the burner length. Proper exposure of the film is achieved by selecting an appropriate shutter speed and f/stop combination which align the camera's meter and aperture needles. Values of shutter speed and f/stop can be used together as a measure of relative flame luminosity:

$$RL = \text{Relative Flame Luminosity} = (\text{shutter speed} \times \text{aperture area})^{-1},$$

where

$$f/\text{stop} = \frac{\text{focal length}}{\text{aperture diameter}}.$$

Units for RL are $(s\text{-}mm^2)^{-1}$. Luminous yellow flames have high values of RL relative to nonluminous blue flames.

Spectroscopic flame studies were conducted using a laboratory-built spectrograph. The device is built around a 0.25 m Jarrell Ash Model 82-410 monochromator. A 0.23 m focal length first-surface spherical mirror operating in a slightly off-axis configuration focuses incoming light onto the 0.008 cm wide entrance slit. Exposure time is controlled by a shutter in front of the slit.

Spectra are recorded on ASA 3000 Polaroid black and white film. The film holder is a Polaroid land camera back mounted to guides for lateral movement. Dispersion constants for the instrument were determined experimentally as 0.315 μm/cm and 0.157 μm/cm for high and low blaze gratings, respectively.

Figure 6 shows the two spectrograph positions used to study flame radiation. No exhaust gas sampling was done during these runs.

2.4 Fuels

Three types of liquid fuels were used in experiments: aviation kerosene, aviation kerosene doped with pyridine (C_5H_5N) to 1 percent nitrogen by mass, and Paraho distillate shale oil. Table 1 summarizes the properties of kerosene and shale oil. Both fuels are similar except for the higher concentrations of nitrogen and sulfur in the shale oil.

TABLE 1

Composition of Aviation Kerosene and
Paraho Distillate Shale Oil Used in Experiments.
(Kerosene Analysis from Ref. 2.)

FUEL	AVIATION KEROSENE	PARAHO DISTILLATE SHALE OIL
GRAVITY, API	36.95	37.0
CARBON	86.08% by mass	85.43% by mass
HYDROGEN	13.70% " "	12.14% " "
NITROGEN	0.002% " "	1.19% " "
OXYGEN	0.15 % " "	<0.50% " "
SULFUR	0.07% " "	0.89% " "
BOILING RANGE	455-550°K	430-545°K
HEATING VALUE	43,205 kJ/kg	44,169 kJ/kg

3. EXPERIMENTAL RESULTS

3.1 Flame Luminosity and Hydrocarbon Measurements

Flame luminosity and unburned hydrocarbons were measured for a wide range of burner conditions. Fuel equivalence ratio (ϕ), atomizing pressure (ΔP), and inlet air preheat temperature were varied independently. The fuel used for these runs was aviation kerosene. Specifically, burner conditions explored included:

$$1.1 \leq \phi \leq 1.9,$$

$$103 \text{ kPa} \leq \Delta P \leq 414 \text{ kPa, and}$$

$$\text{Inlet Air Preheat} = 300, 450, 600°K.$$

Figures 7 through 9 are displays of flame photographs for different preheat temperatures. Each display shows the effect of equivalence ratio and atomizing pressure on unburned hydrocarbons (HC) 5.0 diameters downstream and relative flame luminosity (RL).

Each flame survey is divided diagonally into a nonluminous blue and a luminous yellow region. Blue flames are characterized by CH band spectra and CO continuum radiation while yellow flames are evidence of thermal radiation from soot [1]. Compared to yellow flames, blue flames have lower values of RL. All blue flames at a particular preheat temperature have values of RL within a factor of 2. Yellow flames may have values of RL which differ by a factor of 20 or more. At each preheat temperature for any equivalence ratio less than 1.7, an increase in atomizing pressure causes the flame to change from yellow to blue. Simultaneously, RL and HC decrease as atomizing pressure is increased. Yellow flames, high HC, and high RL persist at the extremely fuel-rich condition $\phi = 1.9$ throughout the entire range of atomizing pressure.

Comparison between Figures 7, 8, and 9 shows a shift in the blue flame region to lower atomizing pressures as inlet air preheat is increased. At any fixed equivalence ratio and atomizing pressure, HC is lowest at 600°K. Blue flames at 600°K preheat have slightly

higher RL than corresponding flames at the lower preheats. This result is probably due to increased wall radiation at the higher temperature rather than any significant luminosity change of the flame.

Plots were constructed to further explore the dependence of HC and RL on burner parameters. Figure 10 shows the dependence of HC on equivalence ratio for a family of atomizing pressure curves at each preheat temperature. Solid and open symbols represent yellow and blue flames, respectively. In the 300°K case, HC increases steadily with increases in equivalence ratio for each atomizing pressure. At 600°K for atomizing pressures of 241 and 345 kPa, HC stays at a plateau for initial increases in equivalence ratio until some critical value. Beyond this critical equivalence ratio, HC increases rapidly for any further increase in equivalence ratio. The 450°K preheat temperature curves exhibit a combination of the behavior observed at 300 and 600°K. The plateau part of each HC vs. ϕ curve is comprised of blue flames while the increasing part is characterized by yellow flames. The critical equivalence ratio at which the onset of significant hydrocarbons occurs appears to be a function of both atomizing pressure and inlet air preheat. Increasing preheat temperature and atomizing pressure delays the onset of significant hydrocarbons to higher equivalence ratios. In the 300°K preheat case, the HC vs. ϕ curves have no plateau; hence, the onset of HC has already occurred at lower equivalence ratios. Clearly in the 450 and 600°K cases for ΔP = 345 kPa, the onset of hydrocarbons does not occur until ϕ = 1.5.

Figure 11 is a plot of relative flame luminosity as a function of equivalence ratio. These curves appear similar to those presented in Figure 10. For all preheats at a low atomizing pressure of 103 kPa, RL increases to an upper plateau as equivalence ratio is increased. This upper plateau could be the black body radiation limit for the particular size soot particles in the burner. Also, the 345 kPa atomizing pressure curves exhibit a lower plateau at which RL remains constant with equivalence ratio until some critical value. Beyond the critical equivalence ratio, RL increases rapidly. This behavior is exhibited by plots of soot loading as a function of equivalence ratio [3]. As before, the lower plateau occurs for blue flames while the increasing part occurs for yellow flames. For nonluminous blue flames, wall radiation is probably a substantial part of measured

RL. This would explain the slight differences in RL corresponding to the lower plateau at different preheats. Recall in Figure 10 for HC vs. ϕ , the lower plateau on hydrocarbons was relatively insensitive to preheat temperature.

The critical equivalence ratio at which the flame becomes luminous (i.e., onset of soot) is 1.5 for ΔP = 345 kPa at 300°K preheat and 1.7 for ΔP = 345 kPa at 600°K. Poor mixing conditions such as ΔP = 103 kPa suggest the onset of soot has occurred for $\phi <$ 1.1. The intermediate atomizing pressure 241 kPa shows the onset of soot to occur early for 300°K and 450°K preheat. At 600°K, the onset of soot does not occur until $\phi \simeq$ 1.5. It appears that increased preheat delays both hydrocarbon breakthrough and the onset of soot. Higher atomizing pressure effectively moves the appearance of any noticeable soot to higher equivalence ratios.

Figure 12 shows the effect of atomizing pressure on hydrocarbon concentration. For all three preheats at ϕ = 1.1, HC is small ($\simeq$ 5 ppm) and remains nearly constant with atomizing pressure. For ϕ = 1.3 and ϕ = 1.5, HC decreases to lower plateaus. The plateaus occur for those flames which have transitioned from yellow to blue. The levels of the plateaus are different for ϕ = 1.3 and ϕ = 1.5 in the 300°K preheat case. At both 450 and 600°K preheat, the two equivalence ratios have the same plateau. Higher preheat temperature shifts the left edge of the plateau to lower atomizing pressures.

At ϕ = 1.7 and ϕ = 1.9, high values of HC persist throughout the entire range of atomizing pressure. Notice for these equivalence ratios most flames observed were luminous yellow.

Figure 13 shows the effect of atomizing pressure on relative flame luminosity. Once again, there is similarity between the shapes of these curves and those in Figure 12. For equivalence ratios from 1.1 to 1.7, RL is reduced to a plateau as atomizing pressure is increased. This lower plateau appears to be a function of equivalence ratio for 300°K preheat, but it is nearly independent of equivalence ratio for the 450°K and 600°K preheats. Unlike the case of HC vs. ΔP, the lower RL plateau occurs for both blue and

somewhat luminous flames. The shift upward in the lower RL plateau as preheat temperature is increased indicates wall radiation accounts for a substantial part of measured RL at these conditions. Equivalence ratio 1.9 is characterized by high RL for all atomizing pressures which again is probably the black body radiation limit.

3.2 Flame Spectroscopy

Spectroscopic studies were conducted to determine which species present in the combustion gases could be identified. Spectra were recorded looking both axially and radially into the burner. Equivalence ratios explored were 1.1 and 1.5 for atomizing pressures of 103 and 345 kPa. Inlet air preheat was held at 300°K. Kerosene, nitrogen-doped kerosene, and shale fuels were used. This test matrix was chosen to see if either gross variation in equivalence ratio or atomizing pressure produced noticeable changes in the presence of species. Highly luminous flames corresponding to low atomizing pressures produced intense continuum radiation which obscured underlying band spectra. Only data for nonluminous flames occurring at higher atomizing pressures are reported here.

In analyzing the spectroscopic work, it is important to acknowledge the presence of underlying continuum spectra associated with black body radiation from soot and walls as well as the $CO + O \rightarrow CO_2 + h\nu$ and $NO + O \rightarrow NO_2 + h\nu$ recombination continua. The CO + O continuum is most intense between 0.35 and 0.50 μm while the NO + O continuum radiates strongest above 0.40 μm into the infrared [5]. Black body radiation is strongest in the infrared.

Figures 14 through 16 are flame spectrograms for aviation kerosene, nitrogen-doped kerosene, and shale oil as seen looking axially into the burner, respectively. The upper spectrum in each figure corresponds to $\phi = 1.5$ while the lower one corresponds to $\phi = 1.1$. The range of wavelength is the same in all cases.

Figure 14 shows CH and C_2 radicals to be prominent radiators along with the usual Na line. Although the OH system at 0.3064 μm is quite strong in flames containing water vapor [5], it is barely visible here due to the insensitivity of the film to ultraviolet light.

Also, no difference was apparent between the spectrum for the two equivalence ratios. The bands appearing in the infrared are second-order spectra of those species already identified at lower wavelengths. Wall radiation is clearly visible along the top and bottom of each spectrum.

Figure 15 shows spectra for a nitrogen-doped kerosene flame. Both NH and CN radiation are visible due to the increased fuel nitrogen. NH is a strong triplet system at 0.3360 μm, but it appears faint because of film insensitivity at this wavelength. One prominent specie known to exist in the flame is NO, but it is not visible here since it radiates in the ultraviolet.

Figure 16 shows the flame spectrum for shale oil. S_2 radiation is visible along with C_2, CH, NH, and CN. This shale oil contains 0.89% by mass sulfur which is most certainly responsible for the S_2 bands.

Figures 17 and 18 are spectrograms taken looking in the radial direction at 1.0 and 1.5 diameters downstream for aviation kerosene. Figure 17 shows C_2 and CH species. The flame appeared blue through the optical port at this location for both ϕ = 1.1 and ϕ = 1.5. The strong continuum radiation in the red end of the spectrum (0.55 - 0.65 μm) of Figure 17 is probably due to emission from the hot opposing wall.

Further downstream at 1.5 diameters, the color of the flame as seen through the port changed from blue to yellow for both ϕ = 1.1 and ϕ = 1.5. Figure 18 shows the associated spectra. Exposure time for Figure 18 is the same as for Figure 17. In Figure 18, nearly all the CH radiation at 0.3872 μm and blue continuum radiation have disappeared. Presumably, both CH and CO species have been substantially oxidized by this time. The yellow color indicates that soot persists. This flame appeared blue when viewed axially. Apparently, the intense blue radiation closest to the nozzle obscures the downstream soot radiation. Further observations proved the blue-yellow transition zone to be a function of atomizing pressure. Decreasing the atomizing pressure to 103 kPa caused the blue zone to collapse, and the entire first section of the burner was filled with a luminous yellow flame.

3.3 Shale Oil Exhaust Gas Analysis

A "spot check" of shale derived fuel was conducted against nitrogen-doped kerosene. The results are tabulated in Table 2.

TABLE 2

Exhaust Gas Species Concentrations for
Pyridine-Doped Kerosene and Distillate Shale Oil.

FUEL	HC (ppm)	O_2 (%)	CO_2 (%)	CO (%)	NO (ppm)	HCN (ppm)	NH_3 (ppm)	SUM FIXED N	% CONVERSION FUEL N TO SUM FIXED N
DOPED KEROSENE (1.0 % N)	150	< 1.0	7.2	13.0	150	220	180	550	31
SHALE OIL (1.19 %N)	90	< 1.0	6.8	12.8	240	395	40	675	31

Equivalence Ratio, 1.5; Atomizing Pressure, 345 kPa; Inlet Air Temperature, 600°K; Distance Downstream, 5.0 Diameters.

Both fuels are comparable in terms of measured percent conversion of fuel nitrogen to the theoretically predicted total fixed nitrogen. However, there is variation between the two fuels in terms of NO, HCN, and NH_3 concentrations. Concentrations of these species are throught to be dependent on the hydrocarbon structure of the fuel [3]. The persistence of unburned hydrocarbons will greatly affect the concentration of HCN relative to NH_3 and NO. Although the fraction of fuel nitrogen converted to fixed nitrogen is the same for both fuels, it is not surprising the distributions of fixed-nitrogen species are different.

4. DISCUSSION AND CONCLUSIONS

4.1 Correlation of Flame Luminosity and Unburned Hydrocarbons

Figures 10 and 13 show relative flame luminosity and unburned hydrocarbons to behave similarly in response to changes in fuel equivalence ratio, atomizing pressure, and inlet air preheat. Increasing inlet air preheat temperature permitted operation of the burner at higher equivalence ratios with minimum unburned hydrocarbons and soot. At 300°K inlet air preheat and 345 kPa atomizing pressure, unburned hydrocarbons became significant for equivalence ratios in excess of 1.3. In Figures 10 and 12, the data suggest at 300°K preheat there can be substantial unburned hydrocarbons present in low luminosity blue flames. HC and soot do not correlate at this preheat temperature although they do at higher preheats. Increasing the inlet air preheat to 600°K suppressed the appearance of hydrocarbons to equivalence ratio 1.5. Similarly, relative flame luminosity (soot) at 300°K preheat and 345 kPa pressure was low for equivalence ratios below 1.5. At 600°K preheat, the onset of soot did not occur until after equivalence ratio 1.7.

Atomizing pressure was found to be important in controlling hydrocarbons and soot. At 600°K preheat, both the onset of hydrocarbons and soot occurred at equivalence ratios less than 1.1 for poor mixing conditions (ΔP = 103 kPa). Enhanced mixing (ΔP = 345 kPa) shifted hydrocarbon breakthrough and incipient soot limit to equivalence ratios 1.5 and 1.7, respectively. However, there appears to be an atomizing pressure above which this effect is negligible.

MacFarlane et al. [6] investigated the effect of flame temperature on soot formation. They found increasing flame temperature to move the first appearance of soot to higher equivalence ratios. However, peak soot concentrations were highest at the elevated flame temperatures. Also, they showed the onset of soot to occur near ϕ = 1.5 for most fuels, but highly aromatic fuels produced measureable soot at lower equivalence ratios.

Relative flame luminosity appears to be an adequate diagnostic for determination of incipient soot equivalence ratio. Whether or not the incipient soot limit is a good indicator of hydrocarbon breakthrough depends on fuel type. In these experiments, the

onset of soot generally occurred at equivalence ratios 13% higher than those where significant hydrocarbons were first observed. Blazowski et al. [3] have shown the incipient soot limit to coincide with hydrocarbon breakthrough for aromatic fuels. Relative flame luminosity would be a good diagnostic for HCN control in the combustion of an aromatic, nitrogen-containing synthetic fuel. Recall that minimum fixed-nitrogen species occurs at the highest equivalence ratio prior to hydrocarbon breakthrough [3]. Previous work done by Foster [2] on the same burner used in these experiments measured fuel nitrogen conversion to be a minimum at an equivalence ratio of 1.5, atomizing pressure of 345 kPa, and inlet air preheat of 600°K.

A plot of unburned hydrocarbons vs. relative flame luminosity was constructed to explore quantitatively any relationship between the two measurements. Figure 19 depicts the relationship. Individual equivalence ratios between 1.3 and 1.7 have points which lie along a line. The extremely fuel-rich condition ϕ = 1.9 and the leaner condition ϕ = 1.1 have points which cluster together.

The cluster of points at ϕ = 1.9 (i.e., one value of RL and one value of HC for all atomizing pressures) suggests the burner is operating in an oxygen-starved condition. Consequently, the equivalence ratio distribution in the burner is uniform, and the process may be kinetically controlled. However, the cluster of points at ϕ = 1.1 suggests mixing at even the lowest atomizing pressure was sufficient to suppress the onset of soot.

There does not seem to be a universal relation between luminosity and unburned hydrocarbons for all equivalence ratios. The effect of changing flame temperature associated with changing equivalence ratio is a complication. Flames at higher equivalence ratios have higher soot loadings; but their mean flame temperatures are lower. Differences in measured RL between equivalence ratios may not be indicative of changes in soot loading. This effect needs further investigation.

4.2 Assessment of Spectroscopic Work

In Section 3, an observation was made concerning the change of flame color from blue to yellow at 1.5 diameters downstream. Reference to the spectra recorded at this

position showed CH band radiation at 0.3872 μm and CO continuum radiation to be less intense than that observed at 1.0 diameter downstream. The yellow color observed 1.5 diameters downstream is probably due to soot radiation.

Pompei [7] has shown CO to decay rapidly between 1.0 and 2.0 diameters downstream in a diffusion flame using exhaust gas sampling. Experiments with other burners have shown soot concentrations to reach a peak between 1.5 and 2.0 diameters downsteam [8,9]. The two processes, CO decay and soot formation, probably occur independent of one another. Acetylene and benzene, known precursors of soot [10], radiate in the ultraviolet below 0.30 μm [5]. It is not until the molecular weight of the soot particles has increased substantially that they radiate as black bodies resulting in the strong continuum radiation in the yellow-red end of Figure 18.

4.3 Conclusions

The data allow the following conclusions to be drawn:

1. Relative flame luminosity is an adequate diagnostic to determine the onset of soot. The onset of soot has previously been shown to be an indication of hydrocarbon breakthrough for highly aromatic fuels.

2. Hydrocarbon concentration appears to be a function of both flame luminosity and equivalence ratio at a fixed inlet air preheat. The exact nature of the relation is uncertain.

3. Both hydrocarbon breakthrough and the onset of soot can be suppressed to higher equivalence ratios by enhanced mixing and higher inlet air preheat. There appears to be an upper limit on the magnitude of the effect.

4. Since hydrocarbon breakthrough usually occurs at leaner equivalence ratios than the onset of soot, minimization of HCN using flame luminosity as a control may not be optimum.

REFERENCES

1. Gaydon, A.G., The Spectroscopy of Flames, Halstead Press, Second Edition, New York, 1974.

2. Foster, D.E., "The Control of NO_x from the Combustion of Fuels with a High Nitrogen Content," Ph.D. Thesis, Department of Mechanical Engineering, M.I.T., November 1978.

3. Blazowski, W.S., Sarofim, A.F., and Keck, J.C., "The Interrelationship Between Soot and Fuel NO_x Control in Gas Turbine Combustors," Paper presented at the ASME Twenty-Fifth International Gas Turbine Conference, March 9-13, 1980, New Orleans.

4. Canon AT-1 Operating Instructions, Canon Publication 1E 1034Q.

5. Pearse, R.W.B., and Gaydon, A.B., The Identification of Molecular Spectra, Halstead Press Division, John Wiley & Sons, Inc., Fourth Edition, New York, 1976.

6. MacFarlane, J.J., Holderness, F.H., and Whitcher, F.S.E., "Soot Formation Rates in Premixed C_5 and C_6 Hydrocarbon-Air Flames at Pressures up to 20 Atmospheres," Combustion and Flame, Vol. 8, 1964, pp. 215-229.

7. Pompei, Francesco, "The Role of Mixing in Burner Generated Carbon Monoxide and Nitric Oxide," M.S. Thesis, Department of Mechanical Engineering, M.I.T., January 1972.

8. Shamsavari, K., "Measurement of Soot in a Turbulent Diffusion Flame", M.S. Thesis, Department of Mechanical Engineering, M.I.T., July 1976.

9. Hoover, J.A., "Soot Production in a Turbulent Diffusion Flame: Turbulent Scaling and Fuel Composition Effects," M.S. Thesis, Department of Mechanical Engineering, M.I.T., June 1978.

10. Prado, G., Lee, M.L., Hites, R.A., Hoult, D.P., and Howard, J.B., "Soot and Hydrocarbon Formation in a Turbulent Diffusion Flame", 16th International Symposium on Combustion, 1976, pp. 649-661.

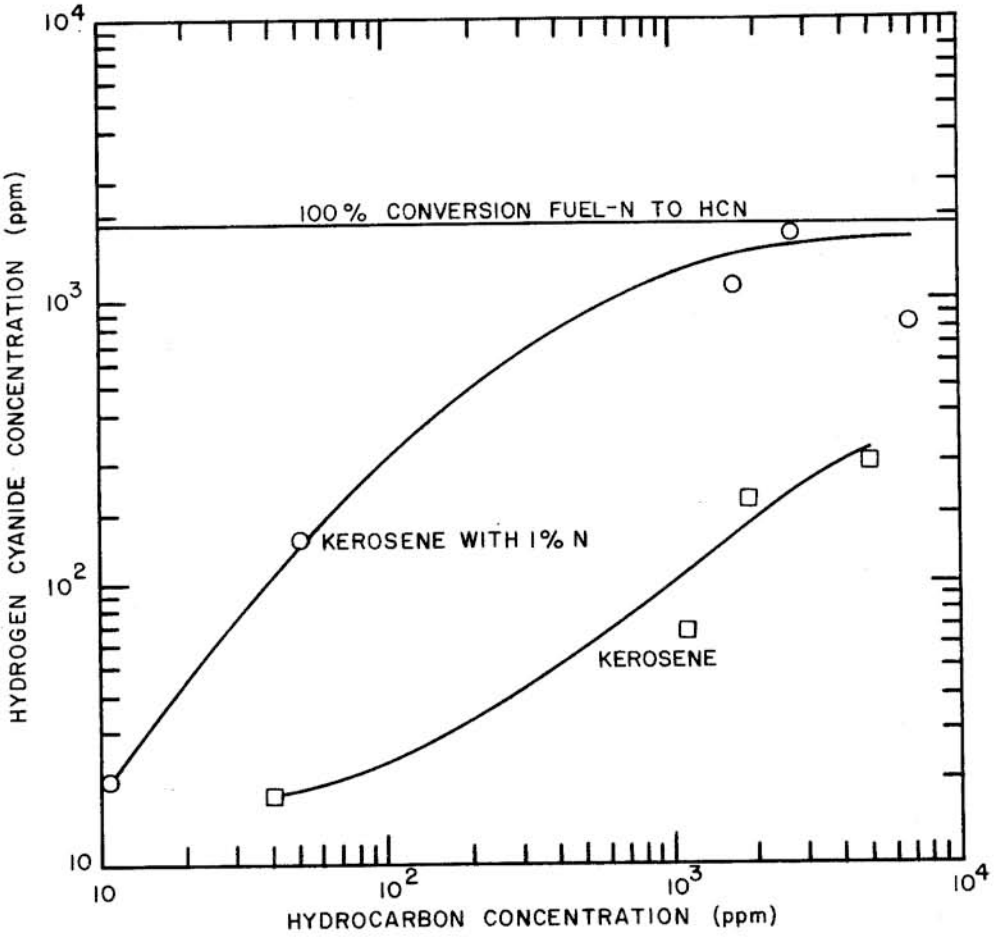

Fig. 1. Variation of Hydrogen Cyanide with Unburned Hydrocarbons. Equivalence Ratio = 1.5; Inlet Air Preheat = 600°K; Distance Downstream = 5.0 Diameters [Ref. 2].

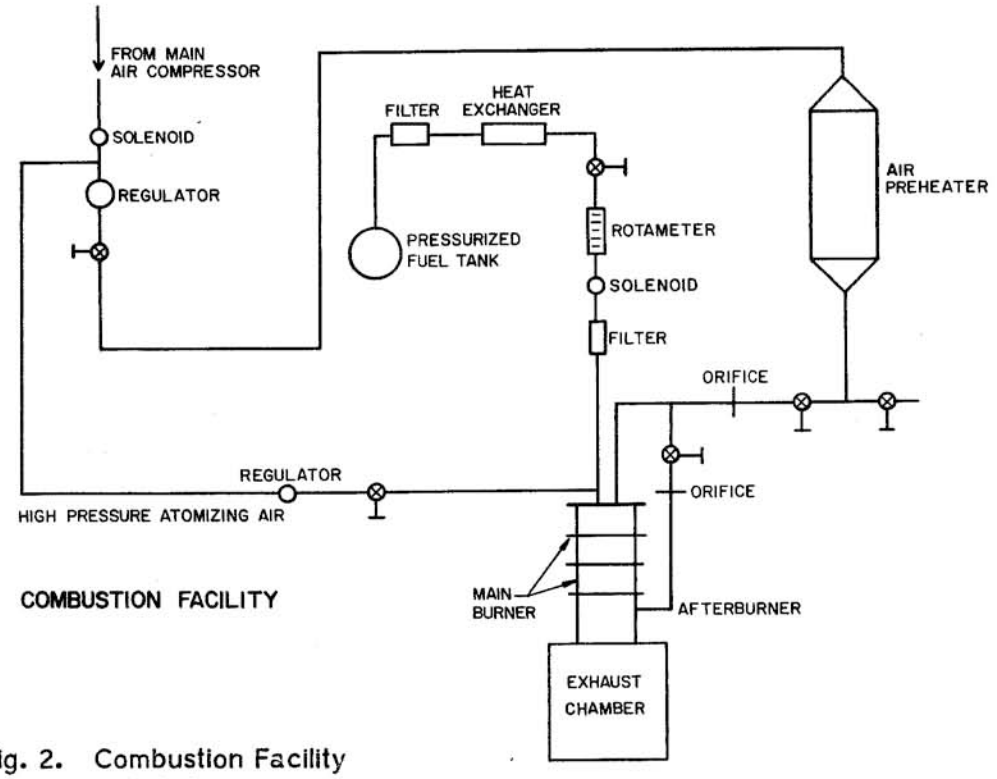

Fig. 2. Combustion Facility Installation.

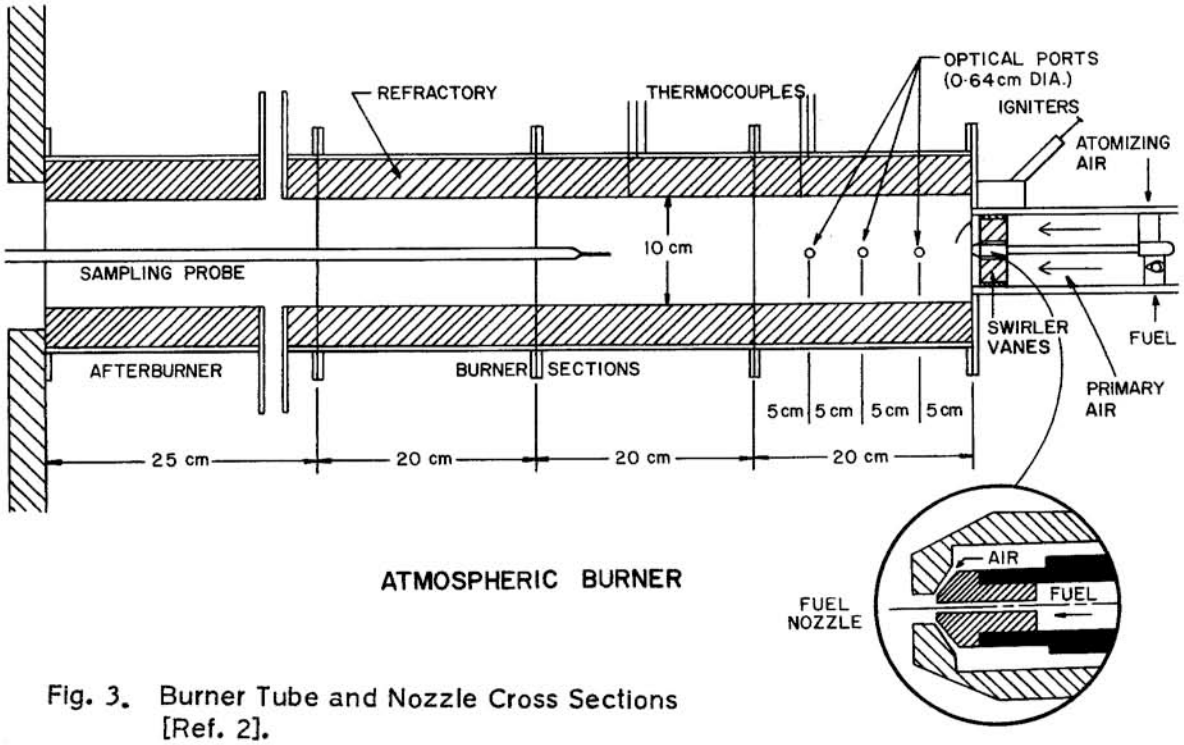

Fig. 3. Burner Tube and Nozzle Cross Sections [Ref. 2].

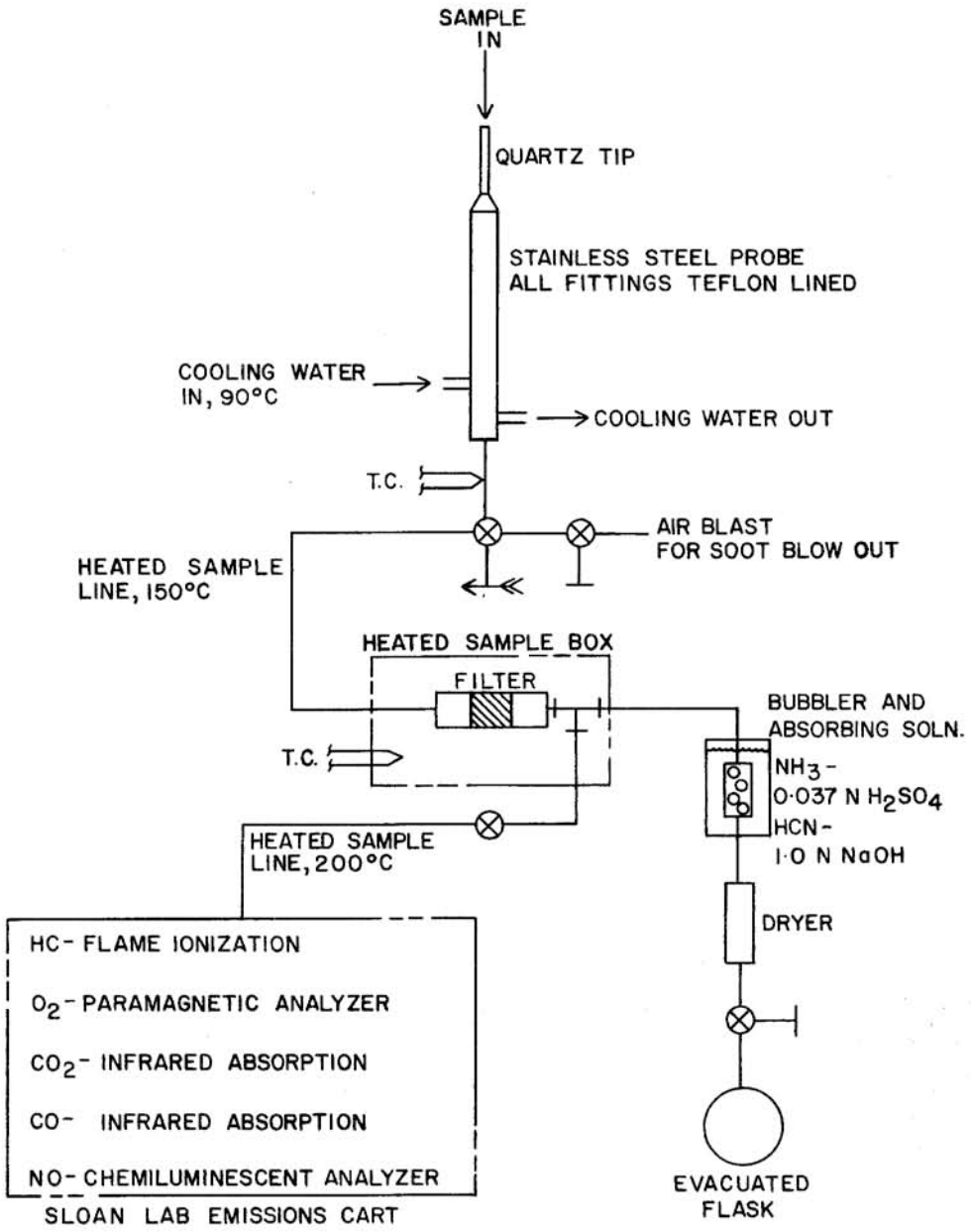

Fig. 4. Complete Exhaust Gas Analysis System Showing Sloan Laboratory Emissions Cart and Wet Chemistry.

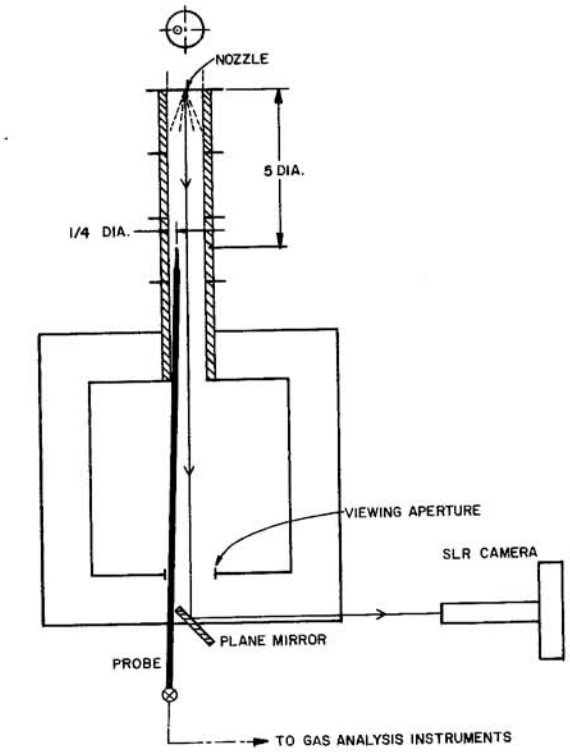

Fig. 5. Experimental Apparatus to Monitor Unburned Hydrocarbons and Flame Luminosity.

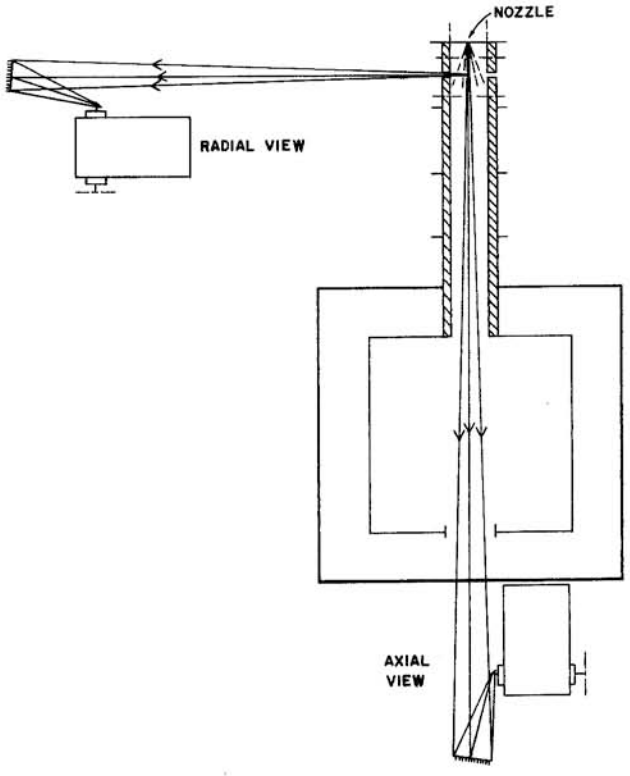

Fig. 6. Spectrograph Positions Used to Study Flame Radiation.

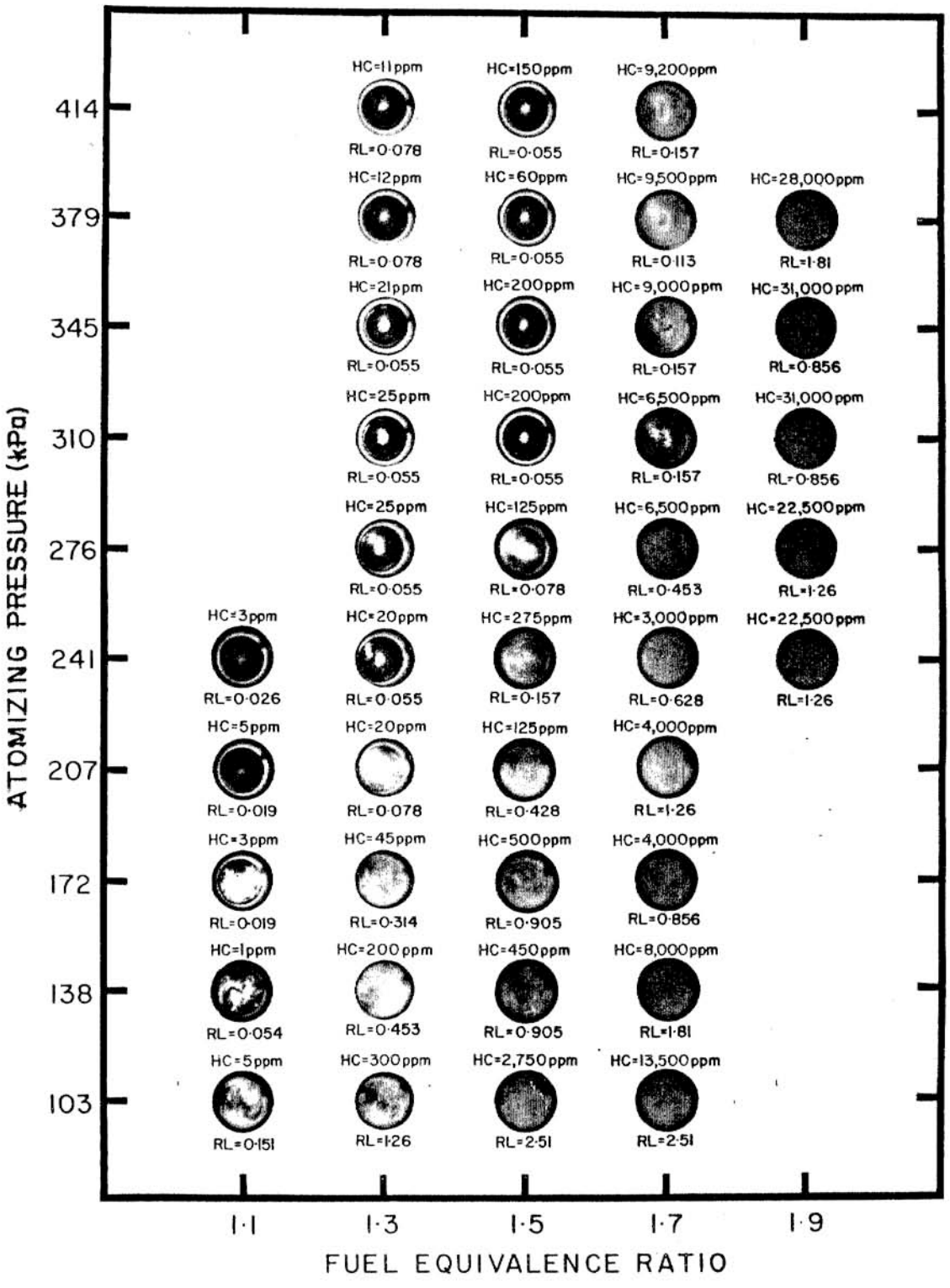

FIG. 7. FLAME PHOTOGRAPHS FOR AVIATION KEROSENE AT 300°K INLET AIR PREHEAT. RL(RELATIVE LUMINOSITY) = (SHUTTER SPEED X APERTURE AREA)$^{-1}$ (s-mm^2)$^{-1}$ FOR ASA 100 KODACOLOR II FILM.

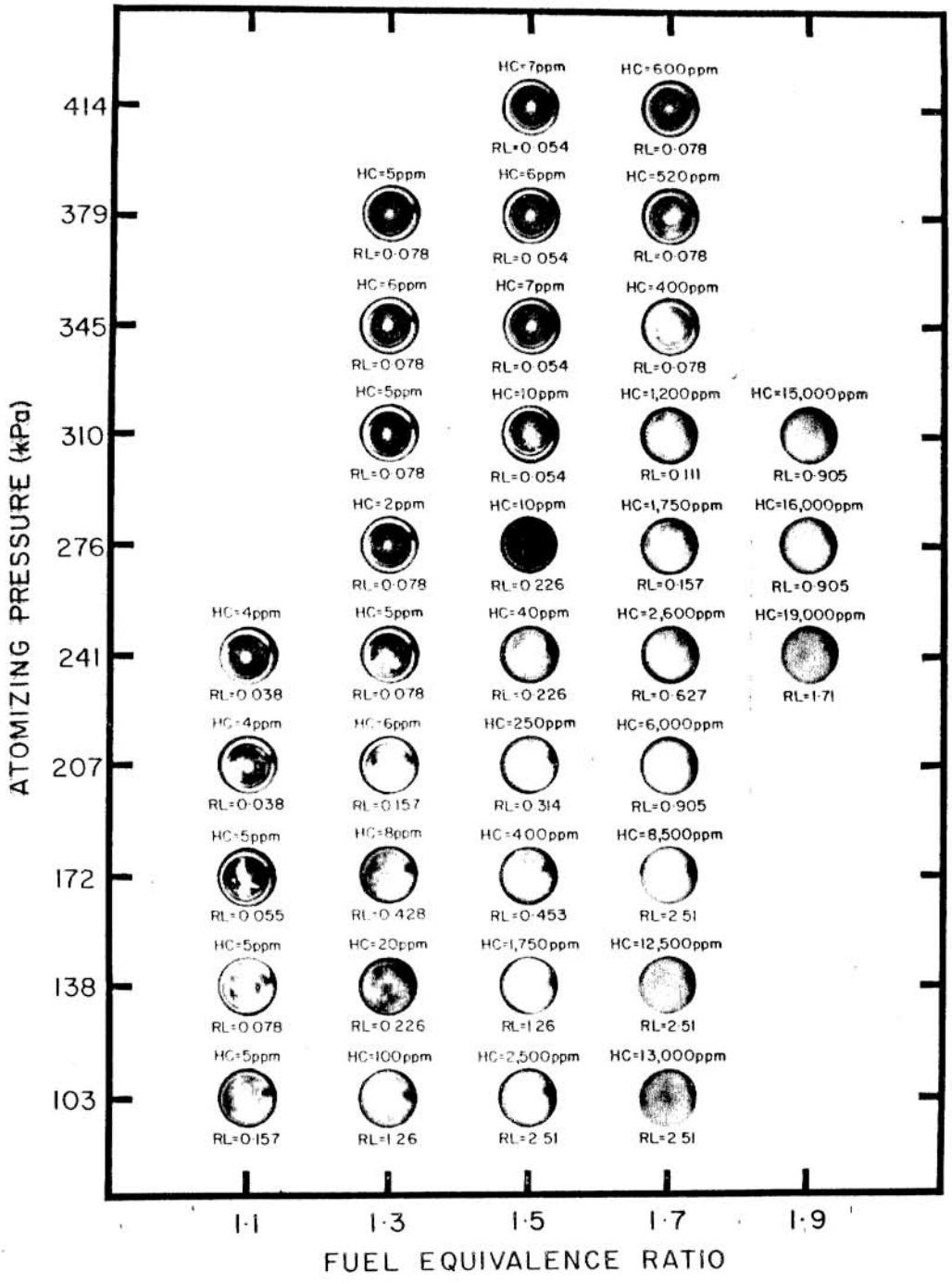

FIG. 8. FLAME PHOTOGRAPHS FOR AVIATION KEROSENE AT 450°K INLET AIR PREHEAT. RL(RELATIVE LUMINOSITY)= (SHUTTER SPEED X APERTURE AREA)$^{-1}$ (s-mm^2)$^{-1}$ FOR ASA 100 KODACOLOR II FILM.

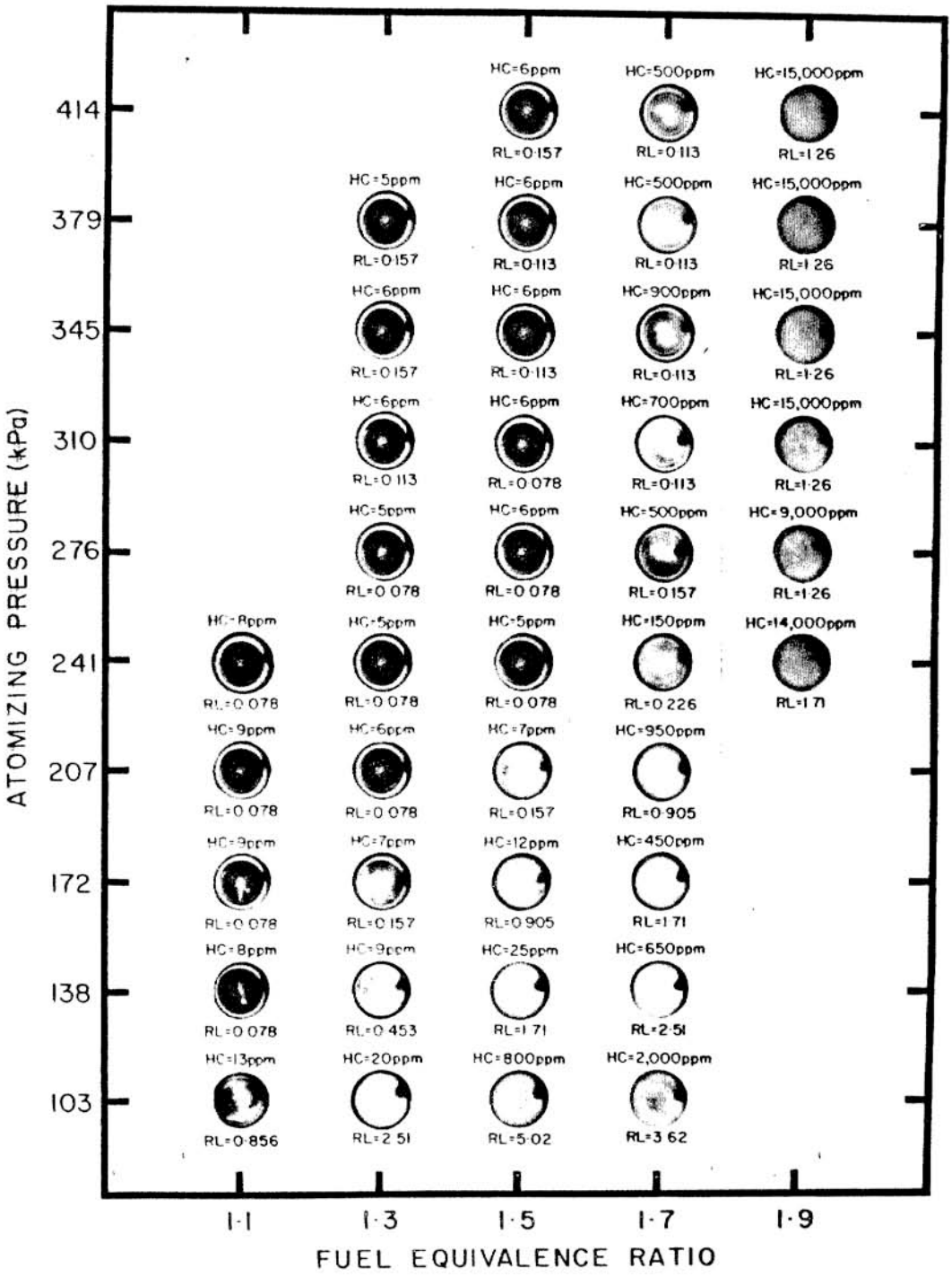

FIG. 9. FLAME PHOTOGRAPHS FOR AVIATION KEROSENE AT 600°K INLET AIR PREHEAT. RL(RELATIVE LUMINOSITY) = (SHUTTER SPEED X APERTURE AREA)$^{-1}$ (s-mm^2)$^{-1}$ FOR ASA 100 KODACOLOR II FILM.

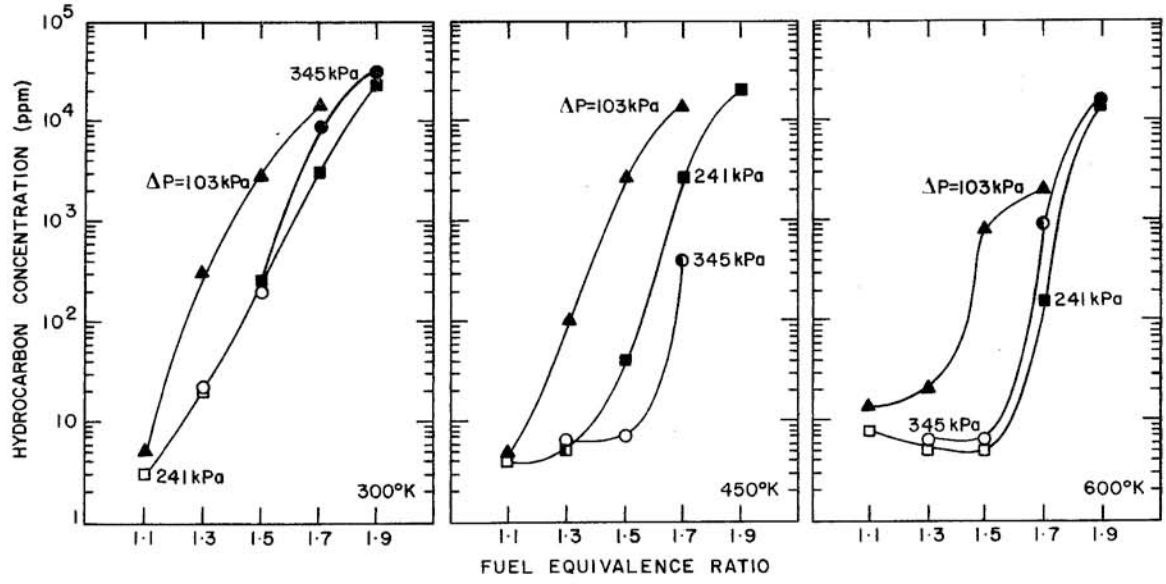

Fig. 10. Unburned Hydrocarbon Concentration as a Function of Fuel Equivalence Ratio for Selected Atomizing Pressures and Inlet Air Preheats. Sample Taken 5.0 Diameters Downstream. Solid Symbol - Yellow Flame; Open Symbol - Blue Flame.

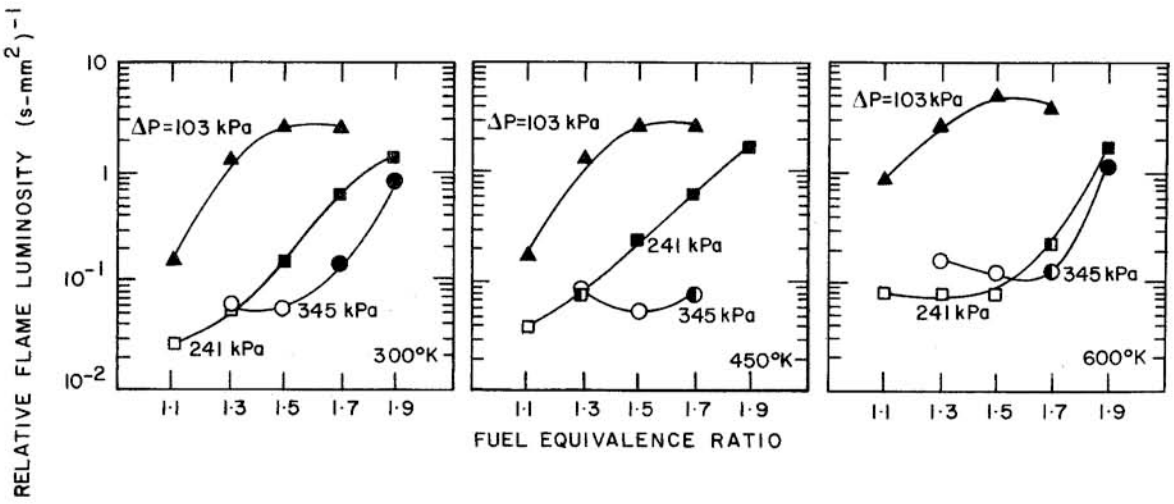

Fig. 11. Relative Flame Luminosity as a Function of Fuel Equivalence Ratio for Selected Atomizing Pressures and Inlet Air Preheats. Solid Symbol - Yellow Flame; Open Symbol - Blue Flame.

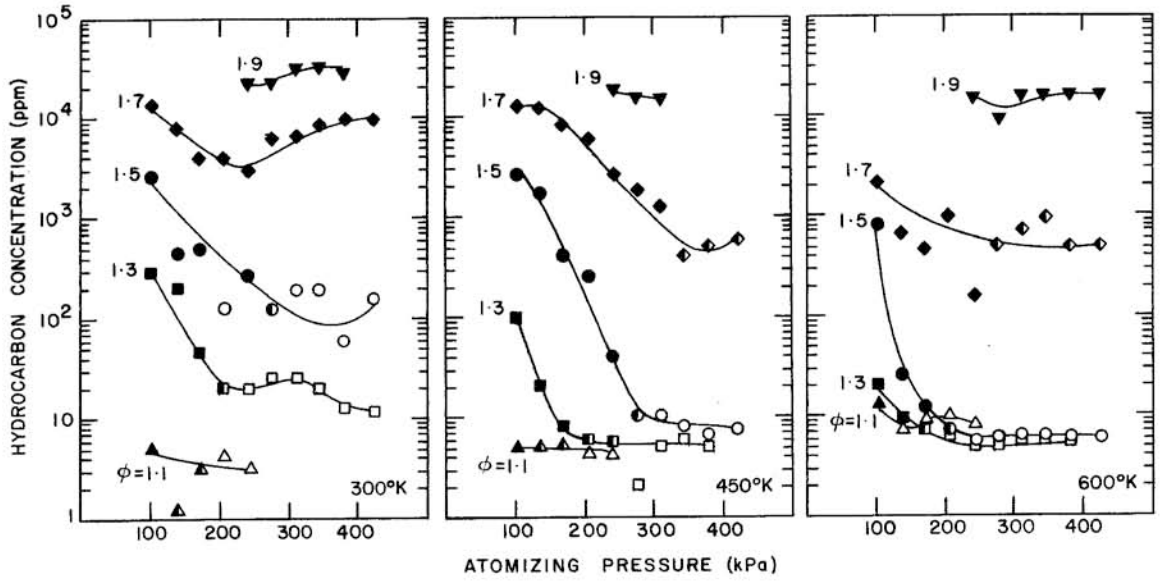

Fig. 12. Unburned Hydrocarbon Concentration as a Function of Atomizing Pressure for Selected Fuel Equivalence Ratios and Inlet Air Preheats. Sample Taken 5.0 Diameters Downstream. Solid Symbol – Yellow Flame; Open Symbol – Blue Flame.

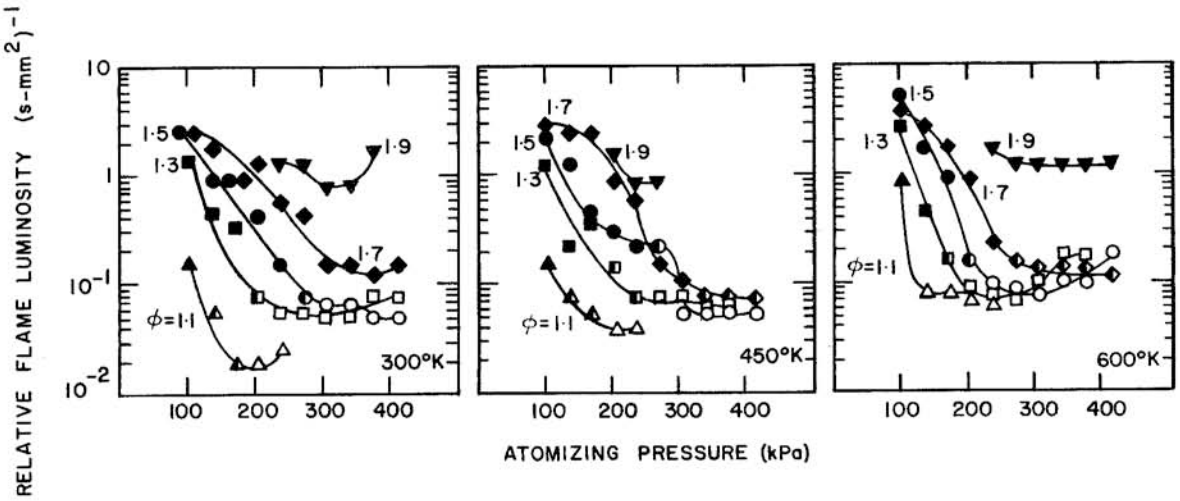

Fig. 13. Relative Flame Luminosity as a Function of Atomizing Pressure for Selected Fuel Equivalence Ratios and Inlet Air Preheats. Solid Symbol – Yellow Flame; Open Symbol – Blue Flame.

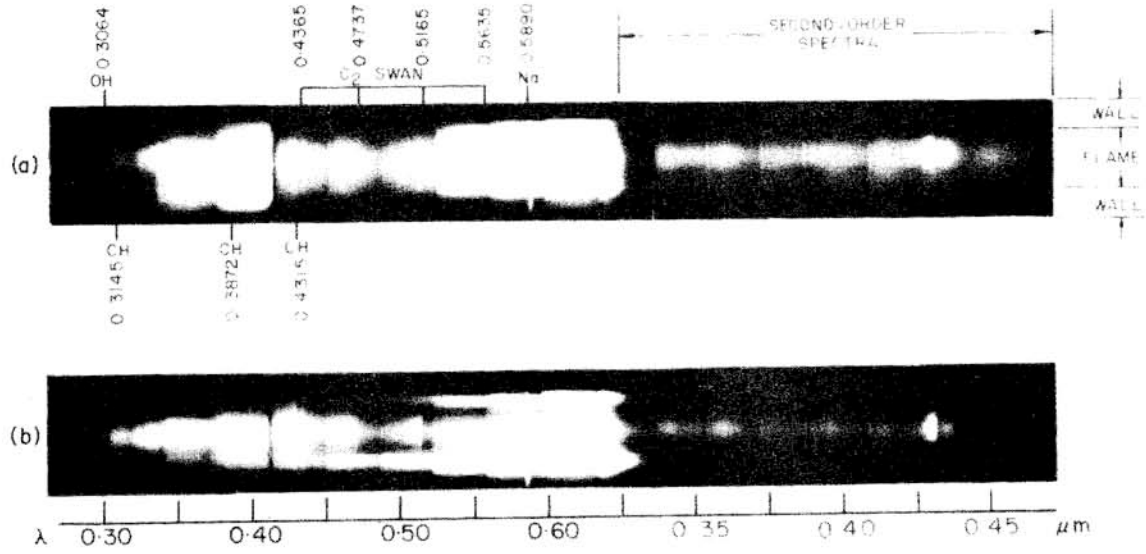

Fig. 14. Flame Spectra for Aviation Kerosene Looking Axially into Burner. Fuel Equivalence Ratios: (a) 1.5; (b) 1.1. Atomizing Pressure = 345 kPa; Inlet Air Preheat = 300°K.

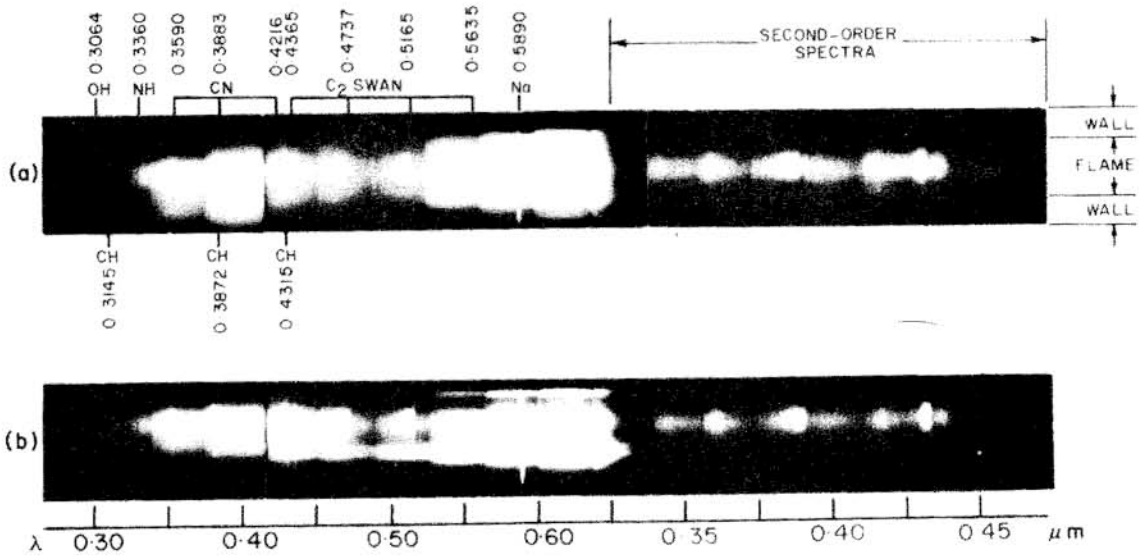

Fig. 15. Flame Spectra for Nitrogen-Doped Kerosene Looking Axially into Burner. Fuel Equivalence Ratios: (a) 1.5; (b) 1.1. Atomizing Pressure = 345 kPa; Inlet Air Preheat = 300°K.

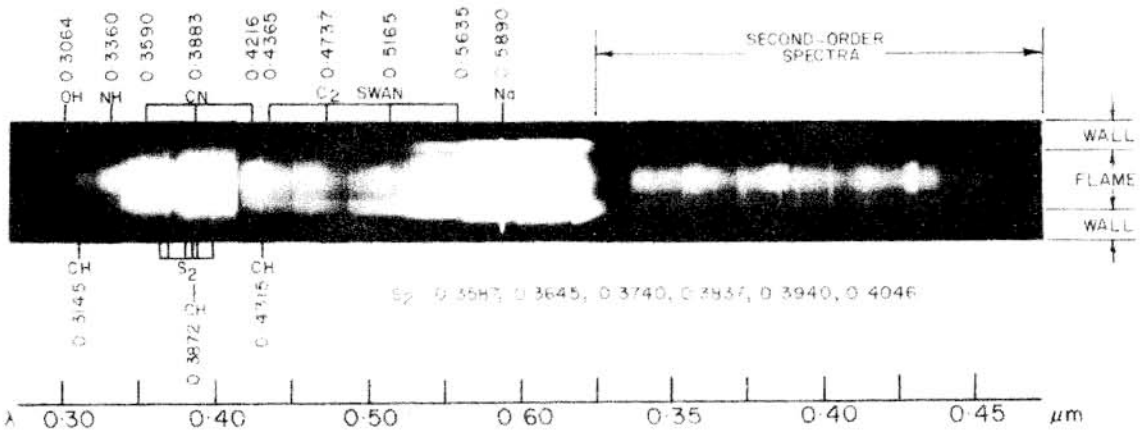

Fig. 16. Flame Spectrum for Shale Oil Looking Axially into Burner. Fuel Equivalence Ratio = 1.1; Atomizing Pressure = 345 kPa; Inlet Air Preheat = 300°K.

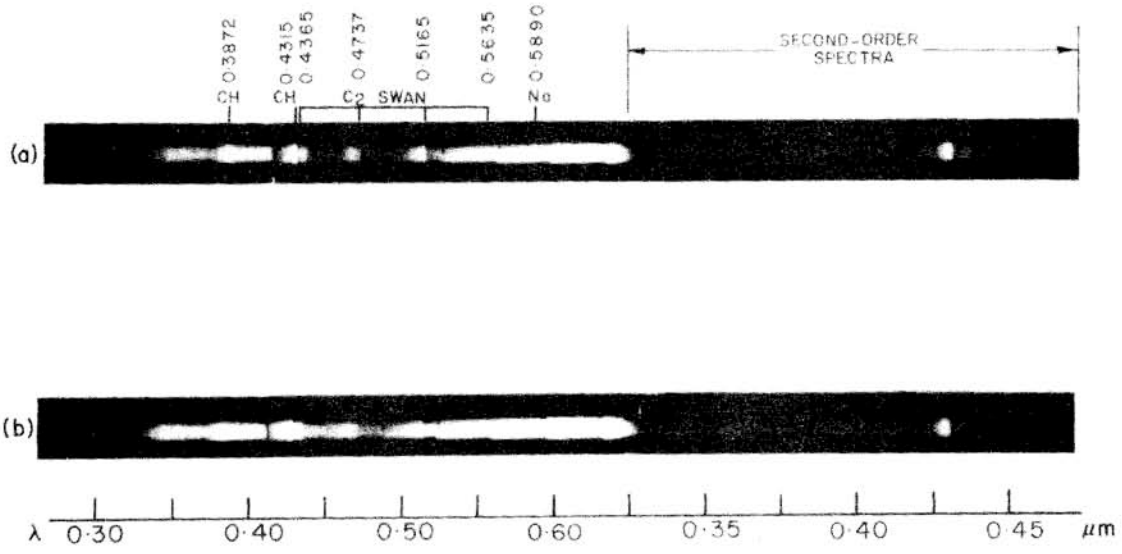

Fig. 17. Flame Spectra for Aviation Kerosene Looking Radially into Burner at 1.0 Diameter Downstream. Fuel Equivalence Ratios: (a) 1.5; (b) 1.1. Atomizing Pressure = 345 kPa; Inlet Air Preheat = 300°K. Flame Appeared Blue to Naked Eye Through Port.

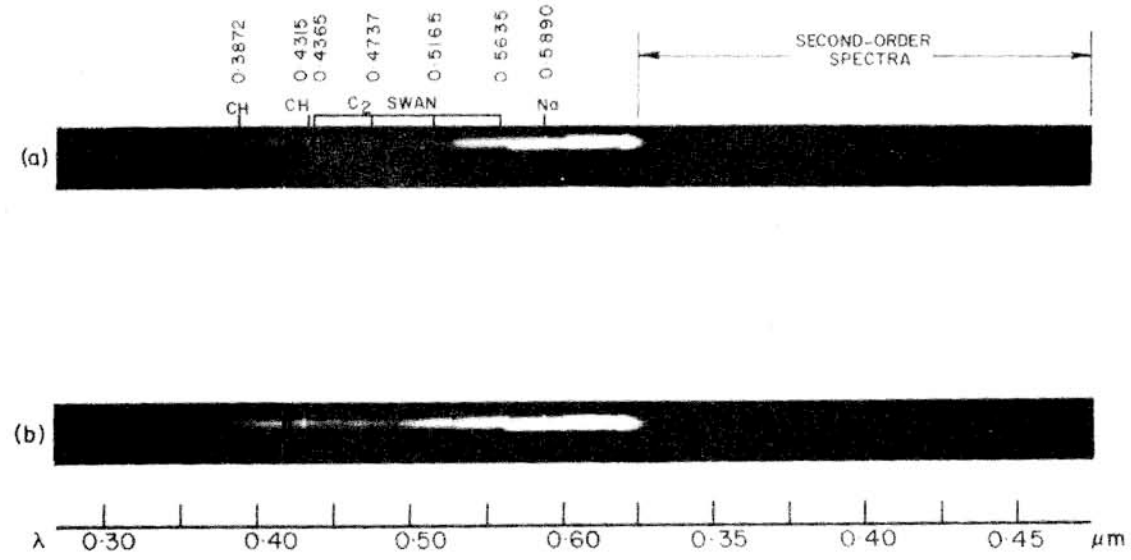

Fig. 18. Flame Spectra for Aviation Kerosene Looking Radially into Burner at 1.5 Diameters Downstream. Fuel Equivalence Ratios: (a) 1.5; (b) 1.1. Atomizing Pressure = 345 kPa; Inlet Air Preheat = 300°K. Flame Appeared Yellow to Naked Eye Through Port.

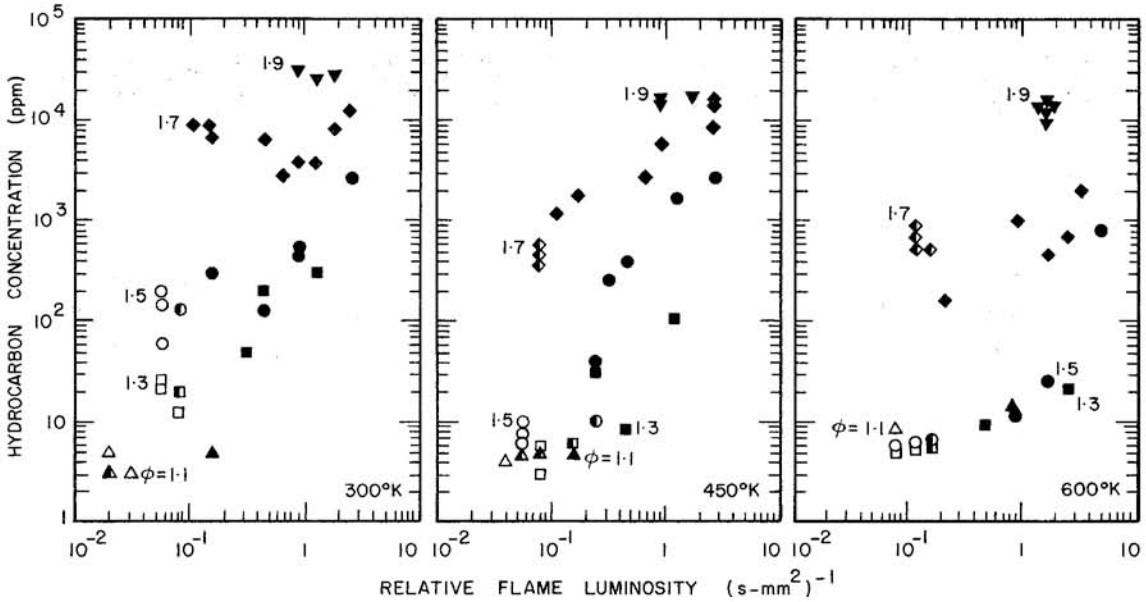

Fig. 19. Unburned Hydrocarbon Concentration as a Function of Relative Flame Luminosity for Selected Fuel Equivalence Ratios and Inlet Air Preheats.

Distribution

J. Birkeland, Division of Power Systems, U.S. DOE
F. Dryer, Princeton University
R. Edelman, Science Applications, Inc., Woodland Hills, CA
A. Ekchian, Massachusetts Institute of Technology
Energy Laboratory Library, Massachusetts Institute of Technology
J. Fischer, Chemical Engineering Division, ANL
D.E. Foster, University of Wisconsin
A. Giovanetti, United Technologies Research Center, East Hartford, CT
A. J. Giovanetti, Massachusetts Institute of Technology
I. Glassman, Princeton University
J. B. Heywood, Massachusetts Institute of Technology
J. D. Hickerson, Pittsburgh Energy Research Center, U.S. DOE
D. P. Hoult, Massachusetts Institute of Technology
Industrial Liason Program, Massachusetts Institute of Technology
B. A. Johnson, Massachusetts Institute of Technology
J. C. Keck, Massachusetts Institute of Technology
S. Lanier, Combustion Research Section, U.S. EPA
D. Latz, Sloan Publications, Massachusetts Institute of Technology
J. M. Levy, Massachusetts Institute of Technology
J. P. Longwell, Massachusetts Institute of Technology
H. V. Messick, Ashland Oil, Inc., Ashland, KY
Patent Counsel, U.S. DOE
R. D. Pierce, Chemical Engineering Division, ANL
S. B. Pope, Massachusetts Institute of Technology
P. C. Powell, Massachusetts Institute of Technology
J. M. Rife, Massachusetts Institute of Technology
H. Ritz, Pittsburgh Energy Research Center, U.S. DOE
L. A. Ruth, Exxon Research and Engineering, Linden, NJ
J. Sangiovanni, United Technologies Research Center, East Hartford, CT
A. F. Sarofim, Massachusetts Institute of Technology (4)
B. R. Taylor, Massachusetts Institute of Technology
Technical Information Center, U.S. DOE (2)
T. Uzkan, International Harvester Co., Hinsdale, IL
D. Whitehead, Ashland Oil, Inc., Ashland, KY